© 2013 by The American Society for Biochemistry and Molecular Biology, Inc.
This paper is available on line at http://www.mcponline.org

Quantitative Phosphoproteomic Study of Pressure-Overloaded Mouse Heart Reveals Dynamin-Related Protein 1 as a Modulator of Cardiac Hypertrophy*[S]

Yu-Wang Chang‡§, Ya-Ting Chang‡§, Qinchuan Wang¶, Jim Jung-Ching Lin¶, Yu-Ju Chen‖, and Chien-Chang Chen‡**

Pressure-overload stress to the heart causes pathological cardiac hypertrophy, which increases the risk of cardiac morbidity and mortality. However, the detailed signaling pathways induced by pressure overload remain unclear. Here we used phosphoproteomics to delineate signaling pathways in the myocardium responding to acute pressure overload and chronic hypertrophy in mice. Myocardial samples at 4 time points (10, 30, 60 min and 2 weeks) after transverse aortic banding (TAB) in mice underwent quantitative phosphoproteomics assay. Temporal phosphoproteomics profiles showed 360 phosphorylation sites with significant regulation after TAB. Multiple mechanical stress sensors were activated after acute pressure overload. Gene ontology analysis revealed differential phosphorylation between hearts with acute pressure overload and chronic hypertrophy. Most interestingly, analysis of the cardiac hypertrophy pathway revealed phosphorylation of the mitochondrial fission protein dynamin-related protein 1 (DRP1) by prohypertrophic kinases. Phosphorylation of DRP1 S622 was confirmed in TAB-treated mouse hearts and phenylephrine (PE)-treated rat neonatal cardiomyocytes. TAB-treated mouse hearts showed phosphorylation-mediated mitochondrial translocation of DRP1. Inhibition of DRP1 with the small-molecule inhibitor mdivi-1 reduced the TAB-induced hypertrophic responses. Mdivi-1 also prevented PE-induced hypertrophic growth and oxygen consumption in rat neonatal cardiomyocytes. We reveal the signaling responses of the heart to pressure stress *in vivo* and *in vitro*. DRP1 may be important in the development of cardiac hypertrophy. ***Molecular & Cellular Proteomics 12: 10.1074/mcp.M113.027649, 3094–3107, 2013.***

From the ‡Molecular Medicine Program, Taiwan International Graduate Program, Institute of Biomedical Sciences, Academia Sinica, Taipei 115, Taiwan; §Institute of Biochemistry and Molecular Biology, School of Life Sciences, National Yang-Ming University, Taipei 112, Taiwan; ¶Department of Biology, University of Iowa, Iowa City, Iowa; ‖Institute of Chemistry, Academia Sinica, Taipei, 115, Taiwan

Received January 25, 2013, and in revised form, July 9, 2013
Published, MCP Papers in Press, July 23, 2013, DOI 10.1074/mcp.M113.027649

Hypertension or acute aortic stenosis causes pressure overload in the left ventricle (LV)[1], and prolonged pressure overload leads to pathological cardiac hypertrophy. Although beneficial initially, hypertrophy in the heart signals metabolic, structural and functional abnormalities and might lead to abnormal cardiac function (1). Patients with LV hypertrophy have increased risk of heart failure, arrhythmia and death (2, 3). Therefore, inhibition of the hypertrophic heart is proposed as a therapeutic target (1, 4). However, one of the major challenges but also the prerequisite to preventing cardiac hypertrophy is a comprehensive understanding of the mechanism to precisely prevent pathologic cardiac growth without affecting homeostasis (1).

The signaling pathways leading to cardiac hypertrophy with chronic pressure overload have been extensively studied by genetic and pharmacological means (1). Proteomic and transcriptomic approaches have been used to study global changes in protein and mRNA expression in hypertrophic hearts (5–7). Acute pressure overload of the heart leads to altered myocardial energy metabolism (8–10) and contractile function (9, 11, 12). However, the signaling pathways contributing to early changes in cardiomyocytes remain unclear.

Protein phosphorylation allows cells to quickly respond to stimuli and transmit signals by regulating enzymatic activity, protein subcellular localization, protein interaction partners, and protein stability (13). Protein phosphorylation is the dominant post-translational modification of cardiac protein (14),

[1] The abbreviations used are: αAR, α-adrenergic receptor; ATP1a1, Na/K ATPase α1A subunit; CV, coefficient of variation; Cryab, αB-Crystallin; DRP1, dynamin-related protein 1; Hspb1, heat shock protein 27; HW/BW, heart weight to body weight; ICAT, isotope-coded affinity tags; ICD, intercalated disc; IMAC, immobilized metal affinity chromatography; iTRAQ, isobaric tag for relative and absolute quantification; LV, left ventricle; LVM/BW, left ventricle mass to body weight; mdivi-1, mitochondrial division inhibitor 1; MS, mass spectrometry; OCR, oxygen consumption rate; Opa1, optic atrophy 1; PE, phenylephrine; PLN, phospholamban; ROS, reactive oxygen species; rNCM, rat neonatal cardiomyocyte; Ryr2, type 2 ryanodine receptor; SERCA2, Sarcoplasmic/endoplasmic reticulum calcium ATPase 2; SR, sarcoplasmic reticulum; TAB, transverse aortic banding.

and many protein kinases and phosphatases are involved in pressure-overload-induced cardiac hypertrophy (1). Abnormal phosphorylation of proteins has been associated with many diseases, including cardiovascular diseases. For example, hyperphosphorylation of type 2 ryanodine receptor (Ryr2) by protein kinase A leads to defective channel function in the human heart (15).

Despite the importance of phosphorylation-mediated regulation in heart diseases, the multiple signaling pathways of cardiac hypertrophy at the phosphoproteome scale have not been delineated. Furthermore, insights into the dynamic interplay of such pathways *in vivo* could greatly enhance our understanding of the molecular mechanism of acute pressure overload and cardiac hypertrophy. In this study, we used quantitative phosphoproteomics to reveal the early signaling pathways induced by acute pressure overload in the mouse LV. Low abundant phosphopeptides were enriched by immobilized metal affinity chromatography (IMAC). To facilitate accurate quantification of phosphorylation *in vivo*, we used a post-enrichment labeling with isobaric tag for relative and absolute quantification (iTRAQ) for quantitative phosphoproteomics and demonstrated reliable quantitation performance with ≈10% coefficient of variation (CV). This strategy provided a large-scale quantification of phosphorylation change of LV proteins at four time points (10, 30, 60 min and 2 weeks) after transverse aortic banding surgery (TAB) in mice. This study revealed potential signal pathways underlying the pressure stress response and the disease phenotypes during the progression of cardiac hypertrophy. We further demonstrated that mitochondrial fission protein dynamin-related protein 1 (DRP1) is involved in the pathological cardiac hypertrophy.

EXPERIMENTAL PROCEDURES

Animal, Transverse Aortic Banding Surgery (TAB), Mitochondrial Division Inhibitor 1 (mdivi-1) Injection, and Echocardiography Analysis—Eight-week-old C57BL/6 male mice (20–25 g) underwent pressure overload by transverse aortic banding (TAB) or sham operation as described (16). For acute TAB, experiments were repeated three times with three mice for each time tested in each replicate (Fig. 1*A*, Exp. Set 1). The hypertrophy experiment involved two replicates with two mice each for TAB and sham operation at 2 weeks in each replicate (Fig. 1*A*, Exp. Set 2).

Mice received an intraperitoneal injection of 25 mg/Kg mdivi-1 dissolved in DMSO every 2 days. Vehicle control mice received an intraperitoneal injection of DMSO every 2 days. Before animals were killed, the pressure gradient across the banding site was checked by echocardiography to ensure the pressure overload (16).

LV Protein Extraction, Mitochondrial Purification, RNA Extraction and Real-Time Quantitative PCR—After the indicated time of TAB, mice were anesthetized for 3 min by isoflurane (3% in oxygen), then killed by neck dislocation. Hearts were excised and weighed, then washed with ice-cold phosphate buffered saline with a phosphatase inhibitor. Atria and right ventricles were removed. The time from neck dislocation to obtain the LV was within 5 min. The LV was frozen by use of liquid nitrogen. For LV protein extraction, 1 ml lysis buffer (20 mM Tris-HCl pH 7.5, 150 mM NaCl, 1 mM Na_2EDTA, 1 mM EGTA, 1% Triton X-100, 2.5 mM sodium pyrophosphate, 1 mM beta-glycerophosphate, 1 mM Na_3VO_4, 1 μg/ml leupeptin) with phosphatase inhibitor mixture (Pierce) was added to each LV for homogenization by use of a Dounce homogenizer (Wheaton). The lysates were incubated on ice for 30 min. Undissolved pellets were centrifuged at 13,000 rpm for 30 min at 4 °C. For mitochondrial isolation, LV was homogenized in buffer containing 250 mM sucrose, 20 mM HEPES pH 7.5, 10 mM KCl, 1.5 mM $MgCl_2$, 1 mM EDTA, protease inhibitor mixture (Sigma) and phosphatase inhibitor mixture. The homogenates were centrifuged first at 800 × *g* for 10 min at 4 °C and supernatant was further centrifuged at 10,000 × *g* for 20 min at 4 °C. The pellets were washed with buffer and spun at 10,000 × *g* for 20 min at 4 °C. The final pellets were dissolved in 1% Triton X-100 lysis buffer. Protein concentrations were determined by the Bradford method (Bio-Rad). Protein lysates were stored at −80 and analyzed within 2 months. Extraction of total RNA from LV and real-time quantitative PCR were as described (16).

Protein Digestion, Phosphopeptide Enrichment, and Isobaric Tag for Relative and Absolute Quantification (iTRAQ) Labeling—For protein digestion, 1 mg LV lysates from each mouse was used, and 0.75 μg α-casein and 0.25 μg β-casein were added. Gel-assisted digestion was used to improve the digestion efficiency of membrane proteins (17). Phosphopeptide enrichment with immortalized metal affinity chromatography (IMAC) was as previously described (18). The IMAC elution was cleaned by use of C18 Ziptip (Millipore). Phosphopeptides were dissolved by use of 10 μl H_2O, and 0.5 μl was added into 100 μl BCA assay reagent (Pierce). The standard curve was created by adding 0.0625, 0.125, 0.1875, 0.25, 0.5, and 1.0 μg BSA into 100 μl BCA assay reagent. After the weight of phosphopeptides was determined, iTRAQ reagent (19) was added to at least twofold the recommended amount. For convenience, 10 μl reconstituted iTRAQ reagent was added into solution containing 9.5 μl phosphopeptides, 2.5 μl TEABC (1 M), and 18 μl ethanol. After 2 h at room temperature, phosphopeptides labeled with different iTRAQ tags were mixed and dried by use of a vacuum pump.

Mass Spectrometry (MS), Database Searching and Phosphopeptide Quantification—Each sample was analyzed at least three times by reverse-phase ultra-performance liquid chromatography (Waters nanoACQUITY UPLC) with quadruple time-of-flight MS (Waters Q-TOF Premier) as described (18). The MS peak lists in Mascot generic format (mgf) were generated by use of Mascot Distiller v2.1.1.0 with default parameters. The combined mgf file was used for a search against the protein database IPI Mouse v3.64 (56,751 protein entries) with an in-house version of Mascot v2.2 (Matrix Science, London, UK). Parameter settings for database searching were trypsin as protease, up to 2 missed cleavages and 0.07 Da for both precursor and fragment ions tolerance. iTRAQ modifications of lysine and N-terminal were set as fixed modification. Methylthio of cysteine, oxidation of methionine, and phosphorylation of serine, threonine, and tyrosine were set as variable modifications.

Proteins were considered identified by significance threshold $p < 0.05$. Peptides were identified by peptide score ≥15. Peptides matched to multiple protein hits were assigned to the protein hit with highest protein score. The false positive rate for peptide identification was 0.62% for acute TAB and 1.46% for TAB at 2 weeks as estimated by Mascot searching against a randomized decoy database. The Mascot delta score was used for phosphorylation site assignment (20). In all, 1,603 MSMS spectra for the 2-week TAB experiment were manually checked. Among 1,462 MSMS spectra with a Mascot delta score ≥ 5 for the first two hits, phosphorylation sites for only one spectrum could not be determined manually. Thus, we used the phosphorylation site assigned by Mascot if the delta score for the first two hits was ≥5.

The quantification of iTRAQ labeling peptide involved use of Multi-Q (21). The mascot protein or peptide identification information was saved as an XML file. The MS and MSMS spectra information

ASBMB MOLECULAR & CELLULAR PROTEOMICS MCP

was converted from Waters (Milford, MA) MassLynx raw data to an mzXML file by use of massWolf software. The XML and mzXML files were loaded into Multi-Q for automatic calculation. The quantifiable MSMS spectra were defined as the peak area of the iTRAQ reporter ion > 25 determined by the 1:1 experiment (supplemental Fig. S2*A* and B).

Three externally added phosphoproteins, bovine α-S1, α-S2 and β-casein, were an internal reference for loss of LV phosphopeptides (supplemental Fig. S2*C*). The reproducibility of quantification for every comparison pair was estimated by the coefficient of variation (CV) of the ratio of casein phosphopeptides in each comparison (supplemental Fig. S3). The LV phosphopeptide ratio was first adjusted by the ratio of casein phosphopeptides, then adjusted by the total peptide ratio to normalize protein loading error. The total trypsin-digested peptide was also labeled with iTRAQ and then analyzed by MS, identified by a database search and quantified by Multi-Q. The signal intensity of the iTRAQ reporter ion for all peptides in each sample was summed and used to normalize the protein input error of each sample. In all, 5204 MSMS spectra were used for quantification. The ratios of MS/MS spectra matched to the same phosphopeptide were averaged. Phosphopeptide ratios of different mice were further averaged and showed as mean ± S.D. The MS/MS spectra are available at http://www.peptideatlas.org/PASS/PASS00236.

GoMiner Analysis, Motif Classification, Cardiac Phenotype Searching, and Hypertrophy Pathway Construction—Subcellular localization and biological processes of phosphoproteins and classes with significant change in phosphorylation were determined by use of the high-throughput GoMiner tool (22). *p* values and FDR for each GO term were calculated, and significance of changes was considered at $p < 0.05$. The classification of phosphorylation sequences by general kinase recognition motifs was as described (23). The cardiac phenotype of phosphoproteins was searched in the Mouse Genome Informatics (MGI) database at *http://www.informatics.jax.org/*. The network of phosphoproteins related to cardiac hypertrophic growth was constructed manually, and the references for events in the network are in supplemental Table S2.

Immunoblotting, Immunofluorescence, and Immunoprecipitation—Samples were incubated with the antibodies for extracellular signal-regulated kinase 1/2 (ERK1/2) T202/Y204, S6 S235/S236, heat shock protein b1 (Hspb1) S82, ATPase α1A subunit (ATP1a1) S16, DRP1 S616, DRP1, protein kinase C δ (PKC-δ), and HA-tag (Cell Signaling Technology); phospholamban (PLN) T17, tubulin, and GAPDH (Santa Cruz Biotechnology, Santa Cruz, CA); mitochondrially encoded cytochrome *c* oxidase (MT-CO1; Abcam, Cambridge, MA); crystallin αB (Cryab) S59 (Enzo Life Sciences, Farmingdale, NY); and α-actinin (Sigma-Aldrich). The mouse Xin antibody clone U1013 was prepared as described (24). Preparation of the rabbit polyclonal phospho-Xin S205/S208 and S295 antibodies involved corresponding synthetic peptides with phosphoserine in the indicated sites. Red fluorescence wheat germ agglutinin (WGA) was from Invitrogen. Immunoblotting, immunoprecipitation, and immunofluorescence were as described (16, 25).

Primary Culture of Rat Neonatal Cardiomyocytes (rNCMs), Transfection, and Measurement of Oxygen Consumption Rate—rNCMs were isolated from ventricles of 1- to 3-day-old rats. The ventricles were digested by use of collagenase and trypsin (Worthington Biochemical Corp, Freehold, NJ) as described (16). Isolated cells were plated in dishes coated with collagen and polylysine (Sigma-Aldrich) in DMEM containing newborn bovine serum (10%), penicillin (100 units/ml) and streptomycin (100 μg/ml) and B-D-arabinofuranoside cytosine (17 μM) for 2 days. After overnight incubation in serum-free medium, rNCMs were treated with PE (10 μM) for 24 h to induce cardiac hypertrophy at 37 °C. The HA-DRP1K38A construct (a kind gift from Dr. Alexander M. Van der Bliek in UCLA) was transfected into rNCMs by use of GeneCellin (BioCellChallenge). The oxygen consumption rate (OCR) of rNCMs (5×10^4/well) was measured by use of a Seahorse XF24 Extracellular Flux Analyzer (Seahorse Bioscience, North Billerica, MA).

Statistical Analysis—Data are presented as mean ± S.E. Statistical comparisons involved Student's *t* test or ANOVA (simple or repeated-measures) and Tukey's post-hoc analysis. A $p < 0.05$ was considered statistically significant.

RESULTS

Quantification of Dynamic Phosphoproteomic Profiles Responding to Pressure Overload in Mice—We used quantitative phosphoproteomics to analyze levels of phosphorylated proteins in LVs of mice to determine protein phosphorylation events within the first hour after TAB-induced pressure overload (Fig. 1*A*). To assure the success of TAB in acute pressure overload, we examined the activation/phosphorylation of ERK1/2 and ribosomal protein S6, known to be acutely phosphorylated in the LV after mechanical stress (25, 26). ERK1/2 was transiently phosphorylated at 10 min after TAB, and S6 was phosphorylated up to 60 min after TAB (supplemental Fig. S1*A*). Early phosphorylation of ERK1/2 and S6 indicated successful induction of pressure overload. The increased ratio of heart weight to body weight (HW/BW) also indicated successful pressure overload with TAB (supplemental Fig. S1*B*).

Temporal responses to pressure overload were analyzed by comparing protein phosphorylation levels at various times after TAB and sham operation (Fig. 1*A*, Exp. Set 1). We also compared levels of cardiac phosphoproteins with chronic pressure overload (2 weeks post-TAB (Fig. 1*A*, Exp. Set 2). We used a post-enrichment iTRAQ labeling strategy and externally added bovine phosphoprotein as a quantification standard. The reproducibility and accuracy of this quantitation strategy was assessed by a 1:1 experiment with four identical LV protein samples (supplemental Fig. S2). With 711 quantifiable phosphopeptides (iTRAQ reporter ion intensity ≥ 25) in the 1:1 experiment, the CV and mean absolute error (MAE) were about 20 and 16%, respectively. The CV and MAE could be reduced to about 10% with reporter ion intensity > 200 for a single phosphopeptide or with number of quantifiable spectra ≥7 (supplemental Fig. S2*B* and *D*). The reproducibility and accuracy of our method were comparable to the quantification of single peptide level by iTRAQ (27). From the 1:1 experiment, we defined a 1.5 fold-change in phosphorylation level as significant difference ($p < 0.05$).

We could quantify 918 unique phosphopeptides from 423 proteins (supplemental Table S1), corresponding to 872 amino acid sites (723 phosphoserines, 111 phosphothreonines, 18 phosphotyrosins and 20 ambiguous sites). In all, 679 phosphopeptides were identified in acute stress, 539 phosphopeptides were identified in chronic stress, and a total of 320 phosphopeptides were consistently identified across all four time points. We determined 164, 110, 121, and 154 differentially regulated phosphorylation sites at 10, 30, and 60 min and 2 weeks, respectively, as compared with sham operation. The overall profiling of protein samples with acute

ASBMB MOLECULAR & CELLULAR PROTEOMICS MCP

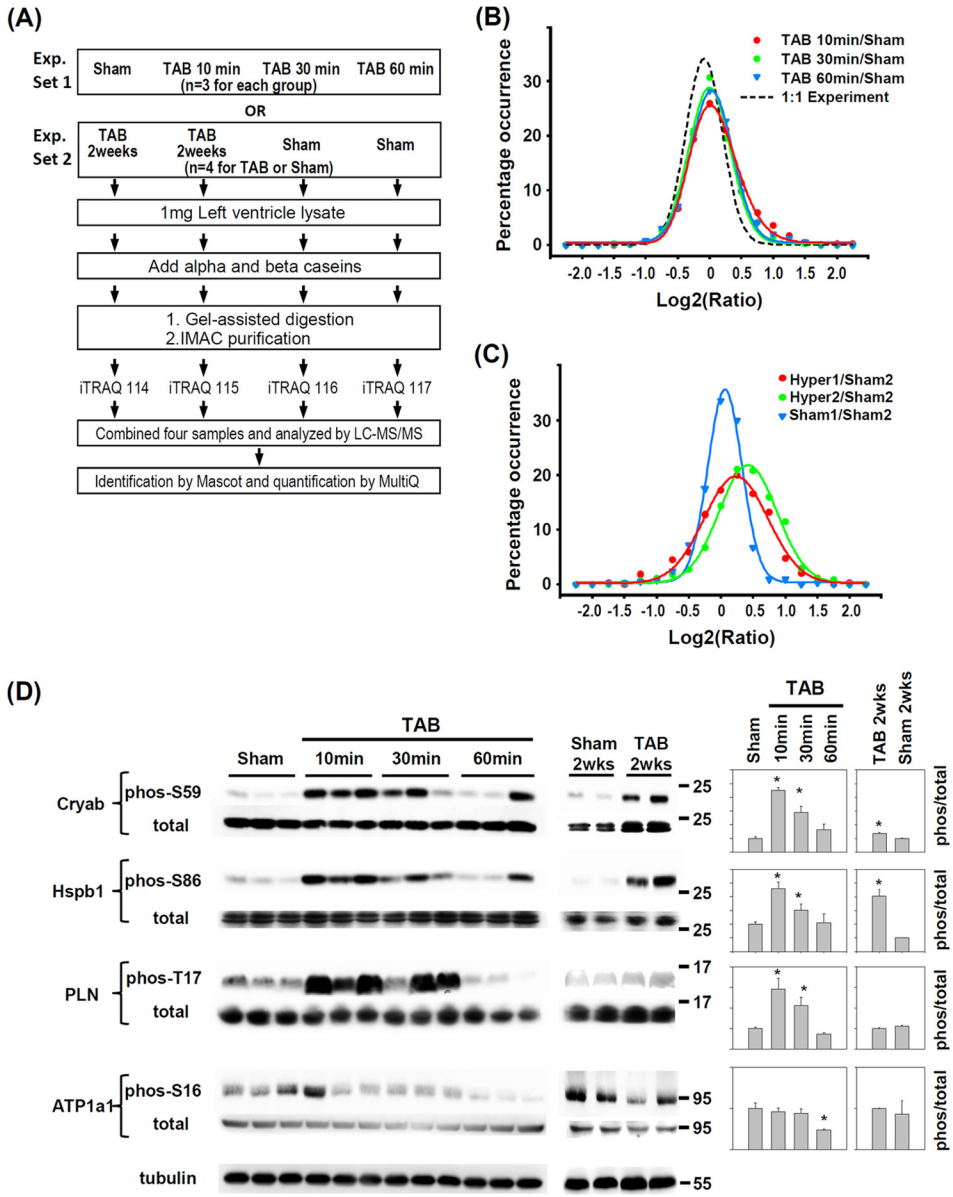


FIG. 1. **Quantitative phosphoproteomics study of pressure-overloaded hearts of mice.** *A*, Strategy for quantitative phosphoproteomic studies of mice with pressure-overloaded hearts induced by transverse aortic banding (TAB). Experimental set 1 (Exp. Set 1) and experimental set 2 (Exp. Set 2) were designed for studying the phosphorylation changes in acute-stressed and hypertrophic hearts, respectively. Phosphopeptide profiles from left-ventricle (LV) tissues of (*B*) acute pressure-overloaded and (*C*) chronic hypertrophic hearts (2 weeks after TAB) as compared with sham-operated hearts. The ratio profile of the 1:1 experiment represents the distribution of unchanged ratios. *D,* Immunoblotting confirmation of regulated phosphorylation sites in αB-Crystallin (Cryab), heat shock protein 27 (Hspb1), phospholamban (PLN) and Na/K ATPase α1A subunit (ATP1a1). Quantification is normalized to total protein. Data are mean ± S.E. * $p < 0.05$ *versus* sham. The position of molecular weight marker is showed to the right of immunoblot.

pressure overload showed a rightward shift as compared with the 1:1 experimental findings (Fig. 1*B*), which indicates an increase in phosphorylated peptides with acute pressure overload. Notably, the analysis revealed a dynamic and transient increase in the profile, which peaked at 10 min post-TAB and was lowest at 30 min post-TAB. The profiles of phosphopeptides with chronic pressure overload also showed a rightward shift as compared with sham operation (Fig. 1*C*).

To assess the biological significant change, we performed Student's *t* test by comparing iTRAQ signal intensities of phosphopeptides between TAB and sham mice. A total of 119 and 124 phosphopeptides for acute pressure overload and hypertrophic hearts have a $p < 0.05$, respectively (supplemental Table S1). We further evaluated the biological reproducibility by correlation analysis of significant changed ratio. The r^2 values were 0.77 and 0.79 for acute

pressure overload and hypertrophic hearts (supplemental Fig. S4).

Validation of Dynamic Phosphoproteomic Profiles Responding to Pressure Overload—Change in contractility is one of the acute responses when hearts are exposed to pressure overload (9, 11, 12). PLN and ATP1a1 are critical for homeostasis of ions, especially Ca^{2+}, and the contractile function of muscle cells (28, 29). We observed increased phosphorylation of PLN T17 and decreased phosphorylation of ATP1a1 S16 in acute pressure-overloaded but not chronic hypertrophic hearts (supplemental Table S1). These changes were further confirmed by incubation with their site-specific phospho-antibodies (Fig. 1*D*). Phosphorylation of the small heat shock protein Cryab on residue S59 is sufficient to mediate its anti-apoptosis function in cardiomyocytes (30). Phosphorylation of another heat shock protein 27 (Hsp27 or Hspb1) on residue S86 inhibits apoptosis (31). We detected and confirmed increased phosphorylation of Cryab S59 and Hspb1 S86 (supplemental Table S1 and Fig. 1*D*) in acute pressure-overloaded and chronic hypertrophic mouse hearts. These results confirmed our phosphoproteomic findings and provide evidence for the protective effect of short-term pressure overload on ischemia-reperfusion injury (32).

Comparison of Phosphoproteome and Previous Proteome and Transcriptome Analyses—Previously, ICAT, iTRAQ and 2-D electrophoresis analyses revealed 152 proteins differentially expressed in hypertrophic hearts (5, 6). Our study revealed only 17 of our 222 differentially phosphorylated proteins among the 152 differentially expressed proteins. In addition, our study revealed only 26 differentially phosphorylated proteins of the 1072 genes previously reported to be differentially regulated in hypertrophy hearts (7). The low rate of overlap demonstrates the unique ability of the phosphoproteomic approach to identify novel phosphorylated proteins as compared with proteomic and transcriptomic approaches. By searching the Mouse Genome Informatics (MGI) database, we compared those mutated genes involved in abnormal cardiac phenotypes with our identified phosphoproteins. We found 81 phosphoproteins associated with abnormal cardiac phenotypes; 44 and 22 showed changes in phosphorylation in acute pressure-overload and chronic hypertrophic hearts, respectively (supplemental Table S3). Thus, the phosphoproteins we identified are indeed important in cardiac functions. The differential phosphorylation of previously unknown sites suggests their novel mechanisms in cardiac functions.

Temporal Specificity of Kinase Recognition Motifs in Response to Pressure Overload—To understand the types of kinases involved in the differential phosphorylation events induced by pressure overload in mice at different times, we classified the quantified phosphorylation sites into three kinase recognition motifs: acidic (*e.g.* CKI, CKII, GSK3), basic (*e.g.* protein kinases A and C, CaMKII), and proline-directed (*e.g.* ERK1/2, p38 MAPK, CDK5). Compared with phosphorylation sites unchanged with TAB, at 10 min, the proportion with preference for the acidic motif was reduced from 36% to 22% and that with preference for the proline-directed motif was increased from 26% to 33%; at 30 min, the proportion with preference for the basic motif was increased from 26% to 36% (supplemental Fig. S5*A*). These results suggest that different kinases were activated at different times after pressure overload. For example, the pSDxD sequence (pS is phosphoserine and x is any amino acid residue) was discovered as a novel motif highly phosphorylated in hypertrophic hearts (supplemental Fig. S5*B*). The pSDxD motif is recognized by casein kinase II (S/TxxD/E), which suggests that the casein kinase II may play important roles in cardiac hypertrophy through phosphorylation of these sites.

Phosphorylation "Hot" Sites Responding to Pressure Overload—To maintain and regulate heart contraction, cardiomyocytes require a specified subcellular structure, including the sarcoplasmic reticulum (SR), contractile fiber, and intercalated disc (ICD) (33). Thus, we also analyzed the subcellular compartments of all quantifiable proteins for those with differential phosphorylation on acute pressure overload using GoMiner (22). Among 8 major subcellular domains, the nucleus had the most phosphoproteins, but the contractile fiber showed the most changes. The average percentage of differentially phosphorylated proteins was 39.3% in these eight subcellular domains but was 60% (21/35) in contractile fiber proteins (Fig. 2*A*). GoMiner analysis suggest that in addition to contractile fiber, the SR membrane, ICD, Z disc, and cell-matrix junction are hot subcellular sites responding to pressure overload stress in the heart (Table I and Fig. 2*B*). Many SR membrane proteins, including Ryr2, sarcoplasmic/endoplasmic reticulum calcium ATPase 2 (SERCA2), PLN and histidine rich calcium binding protein are involved in regulation of calcium transient during heart contraction (34). We also observed differential phosphorylation of Ryr2 (S2808), SERCA2 (S38), and PLN (S16 and T17) (Fig. 2*B*). These phosphorylation sites are important for the functions of these proteins (15, 28, 35), so phosphorylation of SR membrane proteins and contractile proteins may be one of the immediate responses to pressure overload in cardiac myocytes.

Interestingly, three other phosphorylation hot sites—ICD, Z disc, and cell-matrix junction (also named costamere in muscle cells)—are important for sensing mechanical stretch in cardiomyocytes (36). The Z-disc links the contractile fiber to multiple cell-surface protein complexes involving mechanical sensing such as costameres and ICD (36). We found many differentially phosphorylated proteins located within the costameres (dystroglycan S812; tensin 1 S792, T1015; spectrin-β S2340) as well as to the ICD, including catenin protein complex (Xinα S205, S208, S295), tight junction proteins (ZO1 S111) and the gap junction protein (connexin 43 S325, S364) with acute pressure overload (Fig. 2*B*). Interestingly, we have recently shown that loss of Xinα leads to cardiac hypertrophy, cardiomyopathy and conduction defects in mice (24) and that an up-regulation of Xinα at both mRNA and protein levels is

ASBMB MOLECULAR & CELLULAR PROTEOMICS MCP

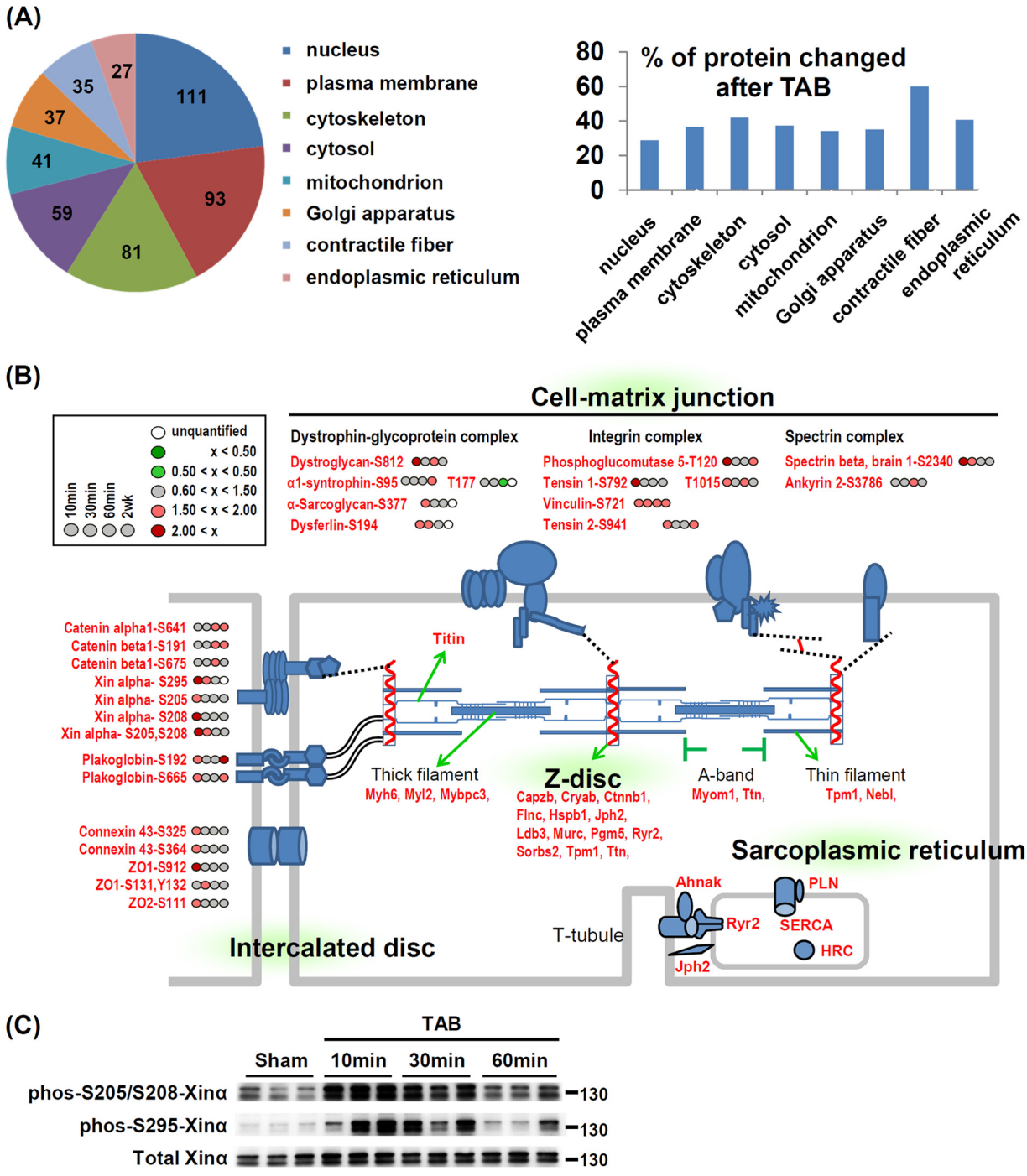


FIG. 2. **Phosphorylation "hot" sites of mouse left ventricles induced by acute pressure overload.** *A*, Classification of quantifiable (pie chart) and differentially phosphorylated (histogram) proteins. Proteins were classified into eight major subcellular compartments according to gene ontology (GO) annotation by use of GoMiner. The number in the pie chart indicates the number of phosphoproteins in each category. The *y* axis of histogram is the percentage of phosphoproteins with changed expression in each compartment. *B*, Enriched phosphorylation changes in mechanical stress-sensing sites: Z-dsic, intercalated disc and cell-matrix junction. The fold change in phosphorylation level of indicated amino acid sites at 4 times after TAB are as in the inset. *C*, TAB-induced phosphorylation of Xinα validated by newly generated phospho-specific antibodies. The position of molecular weight marker is showed to the right of immunoblot.

associated with chronic hypertrophic hearts induced by TAB (37). The phosphorylation of Xinα at S205/S208 and S295 detected in the acute TAB hearts may represent another regulatory mechanism underlying stress-induced cardiac hypertrophy. To confirm our finding of the newly identified phosphorylation sites of Xinα, we generated antibodies against

TABLE I
Enriched gene ontology (GO) terms for phosphorylated proteins differentially regulated in acute pressure-overloaded and hypertrophic mouse hearts

	Acute pressure overload			Hypertrophic heart		
	No. protein[a]	% change	*p* value	No. protein[a]	% change	*p* value
GO cellular compartment term						
Contractile fiber	35	60	<0.05	27	44	0.053
Intercalated disc	9	77	<0.05	9	33	0.51
Sarcoplasmic reticulum membrane	4	100	<0.05	4	25	0.747
Z disc	19	68	<0.05	20	55	<0.05
Cell-matrix junction	11	90	<0.05	11	64	<0.05
Perinuclear region of cytoplasm	25	28	0.809	19	58	<0.05
Cell surface	7	57	0.181	10	70	<0.05
Focal adhesion	8	63	0.092	9	78	<0.05
GO biological process term						
Heart contraction	15	67	<0.05	13	46	0.345
Heart development	17	65	<0.05	12	33	0.718
Carbohydrate metabolic process	20	55	<0.05	27	30	0.86
Cytoskeleton organization	40	48	<0.05	29	45	0.246
Regulation of protein complex disassembly	6	83	<0.05	7	86	<0.05
Lymphocyte activation	7	43	0.444	8	88	<0.05
Cell projection organization	18	44	0.236	18	61	<0.05
Actin filament organization	15	40	0.401	12	67	<0.05
Signal transduction	77	29	0.903	76	41	0.276

[a] Total number of proteins in the category of GO.

phospho-S205/S208 and -S295 Xinα. We confirmed the existence of these phosphorylation events and validated the phosphorylation of the Xinα protein by pressure stress *in vivo* (Fig. 2*C*). These novel findings indicate that the phosphomodulations are launched at multiple mechanical stress sensing sites of cardiomyocytes during acute pressure overload.

Distinct Phosphorylation Patterns Between Acute Pressure-Overloaded and Hypertrophic Hearts—We compared phosphoprotein regulation in hearts with acute pressure overload and chronic hypertrophy. GoMiner analysis of biological processes showed proteins participating in heart contraction, carbohydrate metabolism, cytoskeleton organization, and heart development significantly enriched with acute pressure overload but not hypertrophy ($p < 0.05$, Table I). Because of their roles in heart contraction, proteins located in the contractile fiber, ICD and SR membrane were also significantly changed after acute pressure overload but not hypertrophy (Table I). In contrast, proteins involved in actin-filament organization, lymphocyte activation (including T-cell activation), and cell projection organization (including neuron projection development and axonogenesis) were enriched in hypertrophic but not acutely stressed hearts (Table I). This finding is consistent with T-cell infiltration and sympathetic nerve generation being increased in hypertrophic hearts (38, 39). Our analyses showed that different cellular pathways were activated in cardiac myocytes in response to acute or chronic pressure overload.

Phosphoproteomics Study Suggests a Novel Mediator of Cardiac Hypertrophy—The differentially phosphorylated proteins we identified by our comparative approach allowed us to study their relationship in multiple cellular pathways related to cardiac hypertrophy. A literature search (supplemental Fig. S6; details in Supplemental Table S2) allowed for summarizing these proteins and pathways associated with protein synthesis, glycogen storage, calcium homeostasis, actin polymerization, and cell survival. Our analysis revealed the phosphorylation of many well-known prohypertrophic proteins, such as mammalian target of rapamycin (25) and NF-κB (40). Among those prohypertrophic proteins, PKC-δ showed increased phosphorylation in both acute pressure-overload and chronic hypertrophic hearts (supplemental Fig. S6*A*). Transgene activation of PKC-δ can promote cardiac hypertrophy (41). Interestingly, acute pressure overload increased the phosphorylation of dynamin-related protein 1 (DRP1 S622/isoform1, S596/isoform 2, S579/isoform 3, S491/isoform 4), a PKC-δ substrate, and interacting protein (42) (supplemental Fig. S6*B*, supplemental Table S1). DRP1 is a dynamin-related GTPase and is essential for mitochondrial fission in mammalian cells (43, 44). The phosphorylation status of DRP1 determines its mitochondrial localization and thus mitochondrial fission (45). The phosphorylation of DRP1 S622 by PKC-δ and cdk1/cyclin B promotes mitochondrial fission in neurons (42) and occurs during mitosis in HeLa cells (46). Inhibition of DRP1 has beneficial effects in several disease models (47–50), including reducing ischemia-reperfusion injury in hearts (51). However, whether DRP1 plays a role in the development of cardiac hypertrophy is unknown.

Acute Pressure Overload Induces DRP1 S622 Phosphorylation and Mitochondrial Translocation—To investigate whether DRP1 plays a role in the development of cardiac hypertrophy, we first validated our phosphoproteomic findings by determining the level of DRP1 and phospho-DRP1 (p-DRP1) (S622) after TAB in mice. To confirm the biological reproducibility, the samples we used were independent of the samples used for phosphoproteomics. Level of p-DRP1 from

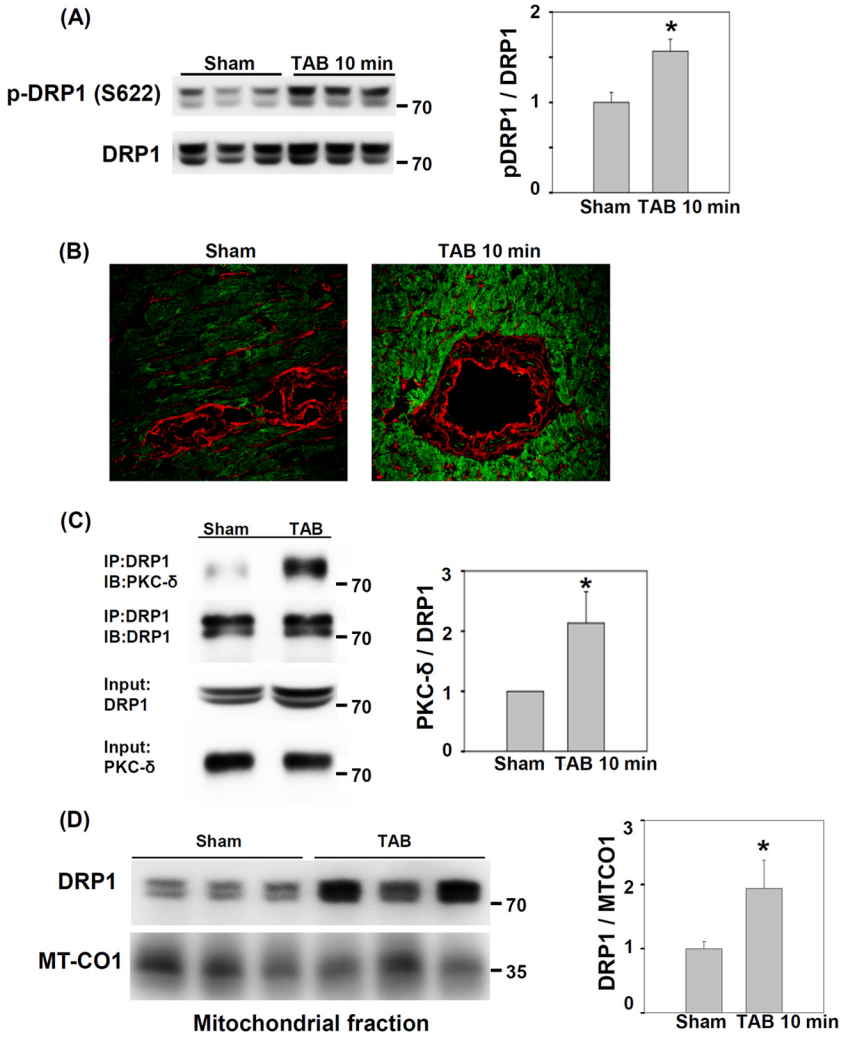


FIG. 3. **Induction of S622 phosphorylation, protein kinase C δ (PKC-δ) interaction and mitochondrial localization of dynamin-related protein 1 (DRP1) by pressure overload in mouse hearts.** *A*, Immunoblotting of phosphorylation of DRP1 S622 in sham-operated and TAB hearts. Data are mean ± S.E. * $p < 0.05$ *versus* sham operation. The position of molecular weight marker is showed to the right of immunoblot. *B*, Immunofluorescence images of phospho-DRP1 S622 in cryosections of LVs from sham-operated and TAB hearts. Green: phospho-DRP1 S622; Red: wheat germ agglutinin for labeling cell-surface glycan. *C*, Co-immunoprecipitation of PKC-δ by anti-DRP1 antibody from LV lysates of sham-operated or TAB mice. LV lysates underwent immunoprecipitation (IP) with anti-DRP1 antibody; PKC-δ and DRP1 were detected by immunoblotting (IB) with their antibodies. Data are mean ± S.E. * $p < 0.05$ *versus* sham operation, $n = 3$. The position of molecular weight marker is showed to the right of immunoblot. *D*, Immunoblotting of DRP1 in the mitochondrial fraction of sham-operated and TAB hearts. Mitochondrial-encoded cytochrome *c* oxidase I (MT-CO1), a mitochondrial marker, was an internal loading control. Data are mean ± S.E. * $p < 0.05$ *versus* sham operation, $n = 3$. The position of molecular weight marker is showed to the right of immunoblot.

LV lysates was increased at 10 min after TAB as compared with sham operation (Fig. 3*A* and 3*B*), with no difference in total DRP1 protein level. Because the interaction between DRP1 and PKC-δ in the brain is increased by hypertension (42), we examined whether the interaction between DRP1 and PKC-δ in the heart changes after acute pressure overload. We found increased level of PKC-δ on co-immunoprecipitation with anti-DRP1 antibody at 10 min after TAB (Fig. 3*C*). Phosphorylation of DRP1 at S622 increases its mitochondrial localization (42). With mitochondrial fractionation, the mitochondrial fraction of DRP1 increased significantly at 10 min after TAB as compared with sham operation (Fig. 3*D*). Thus, acute pressure overload of the mouse heart may promote the interaction between DRP1 and PKC-δ and increase the amount of S622-phosphorylated DRP1 and mitochondrial translocation of DRP1.

Chemical Inhibitor of DRP1 Reduces LV Hypertrophy Induced by Pressure Overload—To investigate the role of DRP1 in the development of cardiac hypertrophy, we treated mice with a chemical inhibitor of DRP1, mdivi-1, before TAB. Mdivi-1 can inhibit the GTPase activity of yeast mitochondrial division dynamin and prevent mitochondrial fission in yeast and mammalian cells (52). Our echocardiography results showed significantly increased ratio of LV mass to body

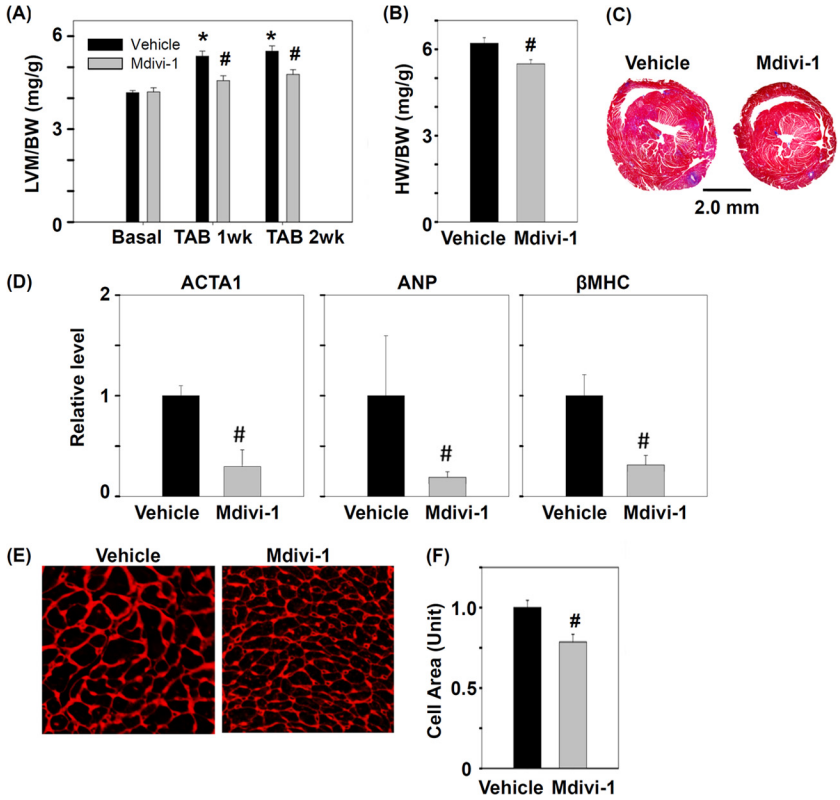


FIG. 4. **Inhibition of DRP-1 alleviates TAB-induced hypertrophy responses in mice.** The ratio of (*A*) LV mass to body weight (LVM/BW) and (*B*) heart weight to body weight (HW/BW) for TAB mice treated with DRP1 inhibitor, mdivi-1, or vehicle. Mdivi-1 (25 mg/Kg) was given by intraperitoneal injection. The LV mass was measured by echocardiography. The heart weight was measured 2 weeks after TAB. * $p < 0.05$ *versus* basal level; # $p < 0.05$ *versus* vehicle group at indicated TAB time; $n = 6$ for vehicle; $n = 7$ for mdivi-1. *C*, Representative sections of vehicle- and mitochondrial division inhibitor 1 (mdivi-1)–treated hearts. Cross sections of hearts were stained with Masson's trichrome 2 weeks after TAB. *D*, Real-time quantitative PCR of mRNA level in vehicle- and mdivi-1-treated hearts with TAB-induced re-expression of hypertrophic marker genes 2 weeks after TAB. Marker genes are atrial natriuretic peptide (ANP), β-myosin heavy chain (βMHC), and skeletal α-actin (ACTA1). Data are mean ± S.E. # $p < 0.05$ *versus* vehicle; $n = 3$. *E*, Cross-sectional area of LV mouse cardiomyocytes 2 weeks after TAB. Sections were stained with WGA to show cell-surface glycan. The surface area of cardiomyocytes was calculated and comparative results are shown in (*F*). Data are mean ± S.E. # $p < 0.05$ *versus* vehicle; $n = 6$ for vehicle; $n = 7$ for mdivi-1.

weight ratio in vehicle-treated mice at 1 and 2 weeks after TAB as compared with mice under the basal condition; however, in mdivi-1-treated mice, the increased ratio was significantly suppressed at 1 and 2 weeks after TAB (Fig. 4*A*). Similarly, HW/BW ratio was significantly lower in mdivi-1- than vehicle-treated mice (Fig. 4*B*, 4*C*). Because cardiac hypertrophy is frequently accompanied by re-expression of cardiac fetal genes (53), we compared the mRNA expression of atrial natriuretic peptide, β-myosin heavy chain and skeletal α-actin in mdivi-1- and vehicle-treated mice with TAB. Compared with vehicle-treated animals, mdivi-1-treated mice showed significantly lower re-expression of these fetal genes (Fig. 4*D*). TAB-induced cardiac hypertrophy results from enlarged individual myocytes, so we examined cross-sectional area of myocytes in the mouse LV and found it significantly smaller in mdivi-1- than vehicle-treated mice at 2 weeks after TAB (Fig. 4*E*, 4*F*). Thus, inhibition of DRP1 with mdivi-1 may ameliorate TAB-induced cardiac hypertrophy.

Inhibition of DRP1 Prevents PE-Induced Hypertrophy in Rat Cardiomyocytes—To determine whether the reduced cardiac hypertrophy observed in mdivi-1-treated mice with TAB was attributable to the direct effect on cardiomyocytes, we isolated and cultured rNCMs and tested their hypertrophic responses to PE *in vitro*. Similar to observations in TAB mouse hearts, level of p-DRP1 (S622) was significantly increased in rNCMs after 1-hr PE treatment (Fig. 5*A*). PE significantly increased the surface area of rNCM (by 32%, $p < 0.001$). However, pretreatment with mdivi-1 blunted the PE-induced increase in cell-surface area (Fig. 5*B*). In addition to pharmacological inhibition, we also downregulated DRP1 activity by transfecting rNCMs with a dominant-negative construct, DRP1K38A (44, 54). Similar to results with mdivi-1, the PE-induced increase in cell-surface area was blunted in DRP1K38A-transfected rNCMs (Fig. 5*C*). Our *in vivo* and *in vitro* studies suggest that DRP1 activity is important in the development of cardiac hypertrophy, and the DRP1 activity inhibitor mdivi-1 may help ameliorate the development of cardiac hypertrophy.

DRP1 Inhibitor Prevents PE-Increased OCR in Rat Cardiomyocytes—Pressure overload affects myocardial metabolism and increases the oxygen consumption of the heart (8, 10).

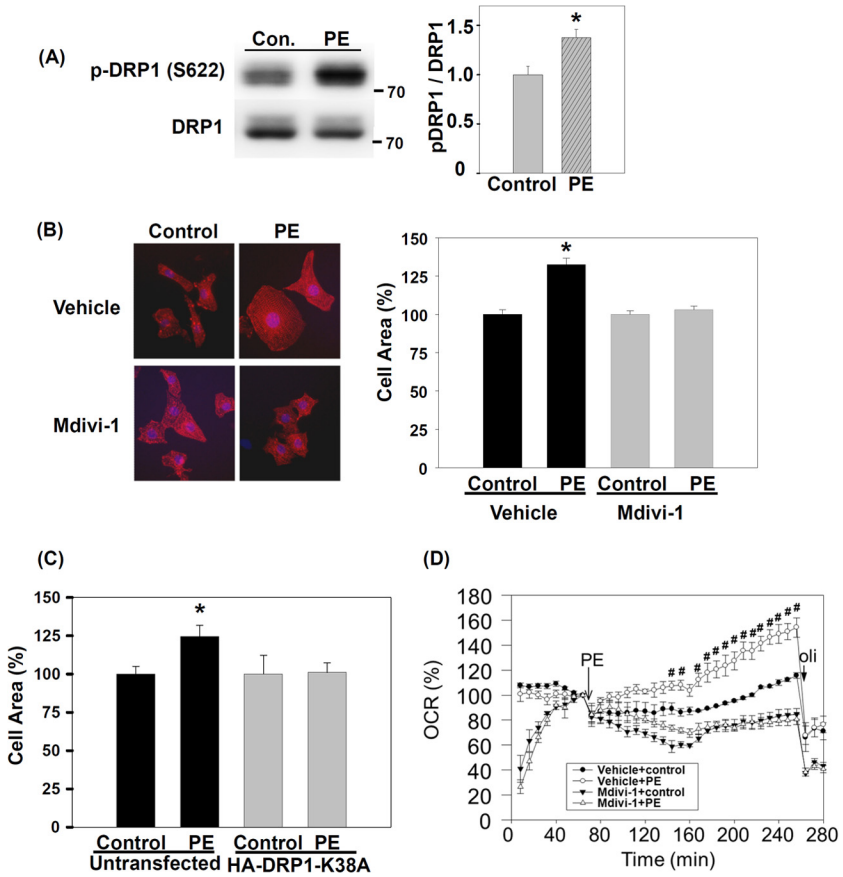


FIG. 5. **DRP1 inhibition prevents phenylephrine (PE)-induced hypertrophic growth and oxygen consumption of rat neonatal cardiomyocytes (rNCMs).** *A,* Phosphorylation of DRP1 S622 in rNCMs after 1 h of stimulation with 10 μM PE. Data are mean ± S.E. * $p < 0.05$ *versus* vehicle; $n = 3$ for each group. The position of molecular weight marker is showed to the right of immunoblot. *B,* DRP1 inhibitor, mdivi-1, prevents PE-induced increase in cell surface area of rNCM. rNCMs were pretreated with 50 μM mdivi-1 or vehicle for 1 h, then treated with 10 μM PE for 24 h. rNCMs were stained with anti-α-actinin antibody (red) and DAPI (blue, for nuclei). At least 100 cells were counted for each group. Data are mean ± S.E. * $p < 0.05$ *versus* control in vehicle. *C,* Transfection of dominant-negative DRP1 prevents PE-induced increase in cell-surface area of rNCMs. HA-tagged dominant-negative mutant of DRP1 (HA-DRP1-K38A) was transfected into rNCMs for 2 days, then rNCMs were treated with PE for 24 h. rNCMs were incubated with anti-HA and anti-α-actinin antibodies. Untransfected groups were cells negative for HA. At least 30 cells were counted for each group. Data are mean ± S.E. * $p < 0.05$ *versus* control in vehicle. *D,* DRP1 inhibitor, mdivi-1, prevents PE-induced increase in oxygen consumption of rNCM. 50 μM Mdivi-1 or vehicle was added to rNCMs 20 min before measurement of real-time oxygen consumption rate (OCR). 10 μM PE and 2 μM oligomycin (oli) were automatically injected into medium at the indicated time. Oligomycin is a mitochondrial ATP synthase inhibitor and is used to estimate the amount of consumed oxygen for ATP synthesis. OCR at each time was normalized to the time just before PE addition. Data are mean ± S.E. # $p < 0.05$ *versus* control in vehicle.

Because DRP1 mediates mitochondrial fission, we examined the impact of DRP1 inhibition on the OCR of rNCMs. PE increases the cellular OCR in hypertrophic rNCMs (55). Mdivi-1 inhibition of DRP1 caused a transient but recoverable reduction in OCR immediately after mdivi-1 treatment (Fig. 5*D*). PE significantly increased the OCR of rNCM but mdivi-1 pretreatment prevented this increase. DRP1-mediated mitochondrial fission may be important for metabolism changes with cardiac hypertrophy.

DISCUSSION

Quantitative Phosphoproteomic Study Reveals the Mechanism of Pressure-Overload-Induced Cardiac Hypertrophy—In this study, we used a MS-based quantitative platform to analyze temporal changes in site-specific protein phosphorylation from murine hearts subjected to TAB-induced pressure overload. This systematic and unbiased approach allowed for revealing multiple mechanisms of responses to pressure-overload stress. For example, we found increased phosphorylation of SERCA2 at S38 and PLN at S16 and T17 at 10 min after TAB. Phosphorylation of these three sites increases the activity of SERCA2 and leads to increased SR calcium reuptake and heart contraction (28, 35). In contrast, phosphorylation of Ryr2 at S2808 was decreased 60 min after TAB. The phosphorylation of Ryr2 at S2808 increases calcium leakage from the SR in failing hearts (15). Our findings suggest that acute TAB could promote SERCA2 calcium reuptake and prevent SR calcium leakage by phosphorylation of regulatory

ASBMB MOLECULAR & CELLULAR PROTEOMICS MCP

ASBMB MOLECULAR & CELLULAR PROTEOMICS MCP

sites of SERCA2, PLN and Ryr2. Interestingly, these changes were not observed in 2-week pressure-overloaded hypertrophic hearts. In addition, we found phosphorylation of α-tropomyosin at T282 and S283 increased in acute pressure-overloaded hearts but decreased in 2-week pressure-overloaded hearts. Dephosphorylation of α-tropomyosin is related to suppression of myocardial sarcomeric tension and ATPase activity in the hypertrophic heart (56). Taken together, these results provide a detailed mechanism of the enhanced contraction function of the heart after acute pressure overload (9, 11, 12).

Here we found phosphorylation changes in heart-contraction, SR-membrane and heart-development proteins with acute pressure-overloaded but not chronic hypertrophic hearts. The absence of these phosphorylation changes in the chronic hypertrophic heart may be because of reduced myocardial wall stress with increased wall thickness of the hypertrophic heart. Another possibility is the additional contraction force provided by the newly synthesized myocardium in the hypertrophic heart. However, we found increased phosphorylation of Cryab S59 and Hspb1 S82 in both acute pressure-overloaded and chronic hypertrophic hearts. The differential phosphorylation events in chronic hypertrophic hearts may be attributed to protein level change, because we and others found the protein level of Cryab up-regulated during hypertrophy (57).

Role of DRP1 in Cardiac Hypertrophy—Our results show that TAB in mice induced DRP1 S622 phosphorylation and mitochondrial translocation. DRP1 S622 can be phosphorylated by PKC-δ (42) or Cdk1/cyclin B (46). In the rat brain, hypertension-induced DRP1 mitochondrial translocation and S622 phosphorylation can be prevented by a PKC-δ inhibitor (42). Increased DRP1 function may be a general response to pressure stress for the brain and heart. In addition, we found that PE, an α-adrenergic receptor (αAR) agonist, could induce DRP1 S622 phosphorylation in cardiomyocytes. Stimulation of αAR by PE causes PKC-δ activation in rNCMs (58). Therefore, TAB-induced pressure overload might trigger the αAR/PKC-δ signal pathway to activate DRP1. Although the activity of Cdk/cyclin B in adult cardiomyocytes is low (59), we cannot rule out that Cdk/cyclin B mediates TAB-induced DRP1 phosphorylation and mitochondrial translocation.

In addition to S622 of DRP1, phosphorylation of S600 by CaMKIIα (60) and ROCK1 (61) and dephosphorylation of S643 by calcineurin (62) also promote DRP1 mitochondrial translocation. Interestingly, CaMKIIα (63), ROCK1 (64), and calcineurin (65) all promote cardiac hypertrophy. DRP1 may be an important convergent point of signaling pathways for cardiac hypertrophy. Determining whether regulation of DRP1 is important for the prohypertrophic activity of these proteins would be of interest.

Our results show that pharmacological and genetic inhibition of DRP1 could prevent cardiac hypertrophy in mice and in rNCMs. The mechanism of this anti-hypertrophic effect may be related to cytosolic calcium and reactive oxygen species (ROS). Recently, DRP1 was shown to mediate the oxygen-induced ductus arteriosus smooth muscle cell (DASMC) contraction and proliferation by increasing cytosolic calcium and ROS (66). Because ROS and calcium are proposed intracellular secondary messengers for cardiac hypertrophy (67–69), TAB may lead to DRP1 activation, which increases intracellular ROS and calcium levels and thus induces cardiac hypertrophy. Another possible mechanism for the involvement of DRP1 in cardiac hypertrophy is the regulation of mitochondrial metabolism. Mdivi-1 inhibits oxygen-induced OCR increase in DASMCs (66). We also showed that mdivi-1 prevented oxygen consumption induced by PE in rNCMs. PE may affect mitochondrial metabolic activity by regulating DRP1 and mitochondrial fission.

Mitochondrial Fission and Fusion Dynamics and Clinical Perspectives for Cardiac Hypertrophy—Our study suggests that regulation of mitochondrial fission proteins may be critical for TAB-induced cardiac hypertrophy in mice. In addition to fission, mitochondrial morphologic features are also controlled by a mitochondrial fusion protein, optic atrophy 1 (Opa1) (45). Opa1$^{+/-}$ mice showed severe pressure-overload-induced cardiac hypertrophy (70). The greater hypertrophy of mice with defective mitochondrial fusion protein is consistent with our finding of less hypertrophy in mice with inhibited mitochondrial fission protein. Mitochondrial fusion proteins may suppress TAB-induced cardiac hypertrophy, but mitochondrial fission proteins may promote it.

Recently, mice carrying a single mutation in DRP1 showed dilated cardiomyopathy and congestive heart failure (CHF) (71). Myocyte hypertrophy was observed in the CHF stage of DRP1 heterozygous mutant mice. This result is in contrast with our finding that inhibition of DRP1 prevented the development of cardiac hypertrophy. One possibility for this discrepancy is that genetic manipulation in mutant DRP1$^{+/-}$ mice may produce developmental defects that differ from that with TAB induction. Inhibition of DRP1 has beneficial effects in several disease models (47–50), including reducing ischemia-reperfusion injury in the heart (51). Our finding that inhibition of DRP1 prevented the development of cardiac hypertrophy is in agreement with these previous studies.

Traditional drug targets of cardiac hypertrophy are cell-surface receptors or ion channels, but the newer drugs target the intracellular signaling pathways, including kinases, phosphatases, and transcription modulators (72). Our phosphoproteomic study revealed novel signaling molecules that could be potential therapeutic targets for intervention in cardiomyopathy. Here, we demonstrated that mdivi-1, a small-molecule inhibitor of DRP1, could suppress pressure-overload-induced cardiac hypertrophy. Thus, DRP1 may be a new therapeutic target in cardiac hypertrophy.

To our knowledge, this is the first phosphoproteomics study to reveal the early response to acute pressure overload in the heart *in vivo*. Most of these dynamically activated or

repressed phosphorylation sites were previously unrecognized to be regulated by pressure overload. This phosphoproteomic approach can reveal the early signal pathways in mechanosensing, metabolism, heart contraction and cardiac hypertrophy during pressure overload of the heart. We also demonstrated that inhibition of the mitochondrial fission protein DRP1 could prevent cardiac hypertrophy in mice and in rat cardiomyocytes. This study broadens our understanding of signaling responses of the heart to pressure stress. As well, interfering in DRP1 function and mitochondrial fission may help control the development of cardiac hypertrophy.

Acknowledgments—We thank the mass spectrometry center of the Institute of Chemistry, Academia Sinica.

* This work was supported by the National Science Council, Taiwan (98-2320-B-001-017-MY3, 100-2311-B-001-002-MY3) and Academia Sinica (AS100-CDA-L05).

[S] This article contains supplemental Figs. S1 to S6 and Tables S1 to S3.

** To whom correspondence should be addressed: Institute of Biomedical Sciences, Academia Sinica, 128 Academia Rd Sec 2, Nankang, Taipei 11529, Taiwan. Tel.: 886-2-2652-3522; Fax: 886-2-2785-8847; E-mail:ccchen@ibms.sinica.edu.tw.

REFERENCES

1. Hill, J. A., and Olson, E. N. (2008) Cardiac plasticity. *N. Engl. J. Med.* **358,** 1370–1380
2. Levy, D., Garrison, R. J., Savage, D. D., Kannel, W. B., and Castelli, W. P. (1990) Prognostic implications of echocardiographically determined left ventricular mass in the Framingham Heart Study. *N. Engl. J. Med.* **322,** 1561–1566
3. Koren, M. J., Devereux, R. B., Casale, P. N., Savage, D. D., and Laragh, J. H. (1991) Relation of left ventricular mass and geometry to morbidity and mortality in uncomplicated essential hypertension. *Ann. Intern. Med.* **114,** 345–352
4. Gardin, J. M., and Lauer, M. S. (2004) Left ventricular hypertrophy: the next treatable, silent killer? *JAMA* **292,** 2396–2398
5. Lindsey, M. L., Goshorn, D. K., Comte-Walters, S., Hendrick, J. W., Hapke, E., Zile, M. R., and Schey, K. (2006) A multidimensional proteomic approach to identify hypertrophy-associated proteins. *Proteomics* **6,** 2225–2235
6. Friehs, I., Cowan, D. B., Choi, Y. H., Black, K. M., Barnett, R., Bhasin, M. K., Daly, C., Dillon, S. J., Libermann, T. A., McGowan, F. X., Del Nido, P. J., Levitsky, S., and McCully, J. D. (2013) Pressure-overload hypertrophy of the developing heart reveals activation of divergent gene and protein pathways in the left and right ventricular myocardium. *Am. J. Physiol. Heart Circ. Physiol.* **304,** H697–708
7. Yang, K. C., Ku, Y. C., Lovett, M., and Nerbonne, J. M. (2012) Combined deep microRNA and mRNA sequencing identifies protective transcriptomal signature of enhanced PI3Kalpha signaling in cardiac hypertrophy. *J. Mol. Cell. Cardiol.* **53,** 101–112
8. Neely, J. R., Liebermeister, H., Battersby, E. J., and Morgan, H. E. (1967) Effect of pressure development on oxygen consumption by isolated rat heart. *Am. J. Physiol.* **212,** 804–814
9. Schwartz, G. G., Steinman, S., Garcia, J., Greyson, C., Massie, B., and Weiner, M. W. (1992) Energetics of acute pressure overload of the porcine right ventricle. In vivo 31P nuclear magnetic resonance. *J. Clin. Invest.* **89,** 909–918
10. Massie, B. M., Schwartz, G. G., Garcia, J., Wisneski, J. A., Weiner, M. W., and Owens, T. (1994) Myocardial metabolism during increased work states in the porcine left ventricle in vivo. *Circ. Res.* **74,** 64–73
11. Chazov, E. I., Pomoinetsky, V. D., Geling, N. G., Orlova, T. R., Nekrasova, A. A., and Smirnov, V. N. (1979) Heart adaptation to acute pressure overload: an involvement of endogenous prostaglandins. *Circ. Res.* **45,** 205–211
12. Dowell, R. T., Cutilletta, A. F., Rudnik, M. A., and Sodt, P. C. (1976) Heart functional responses to pressure overload in exercised and sedentary rats. *Am. J. Physiol.* **230,** 199–204
13. White, F. M. (2008) Quantitative phosphoproteomic analysis of signaling network dynamics. *Curr. Opin. Biotechnol.* **19,** 404–409
14. Van Eyk, J. E. (2011) Overview: the maturing of proteomics in cardiovascular research. *Circ. Res.* **108,** 490–498
15. Marx, S. O., Reiken, S., Hisamatsu, Y., Jayaraman, T., Burkhoff, D., Rosemblit, N., and Marks, A. R. (2000) PKA phosphorylation dissociates FKBP12.6 from the calcium release channel (ryanodine receptor): defective regulation in failing hearts. *Cell* **101,** 365–376
16. Chiang, C. S., Huang, C. H., Chieng, H., Chang, Y. T., Chang, D., Chen, J. J., Chen, Y. C., Chen, Y. H., Shin, H. S., Campbell, K. P., and Chen, C. C. (2009) The Ca(v)3.2 T-type Ca(2+) channel is required for pressure overload-induced cardiac hypertrophy in mice. *Circ. Res.* **104,** 522–530
17. Han, C. L., Chien, C. W., Chen, W. C., Chen, Y. R., Wu, C. P., Li, H., and Chen, Y. J. (2008) A multiplexed quantitative strategy for membrane proteomics: opportunities for mining therapeutic targets for autosomal dominant polycystic kidney disease. *Mol. Cell. Proteomics* **7,** 1983–1997
18. Wang, Y. T., Tsai, C. F., Hong, T. C., Tsou, C. C., Lin, P. Y., Pan, S. H., Hong, T. M., Yang, P. C., Sung, T. Y., Hsu, W. L., and Chen, Y. J. (2010) An informatics-assisted label-free quantitation strategy that depicts phosphoproteomic profiles in lung cancer cell invasion. *J. Proteome Res.* **9,** 5582–5597
19. Ross, P. L., Huang, Y. N., Marchese, J. N., Williamson, B., Parker, K., Hattan, S., Khainovski, N., Pillai, S., Dey, S., Daniels, S., Purkayastha, S., Juhasz, P., Martin, S., Bartlet-Jones, M., He, F., Jacobson, A., and Pappin, D. J. (2004) Multiplexed protein quantitation in Saccharomyces cerevisiae using amine-reactive isobaric tagging reagents. *Mol. Cell. Proteomics* **3,** 1154–1169
20. Savitski, M. M., Lemeer, S., Boesche, M., Lang, M., Mathieson, T., Bantscheff, M., and Kuster, B. (2011) Confident phosphorylation site localization using the Mascot Delta Score. *Mol. Cell. Proteomics* **10,** M110.003830
21. Lin, W. T., Hung, W. N., Yian, Y. H., Wu, K. P., Han, C. L., Chen, Y. R., Chen, Y. J., Sung, T. Y., and Hsu, W. L. (2006) Multi-Q: a fully automated tool for multiplexed protein quantitation. *J. Proteome Res.* **5,** 2328–2338
22. Zeeberg, B. R., Qin, H., Narasimhan, S., Sunshine, M., Cao, H., Kane, D. W., Reimers, M., Stephens, R. M., Bryant, D., Burt, S. K., Elnekave, E., Hari, D. M., Wynn, T. A., Cunningham-Rundles, C., Stewart, D. M., Nelson, D., and Weinstein, J. N. (2005) High-Throughput GoMiner, an 'industrial-strength' integrative gene ontology tool for interpretation of multiple-microarray experiments, with application to studies of Common Variable Immune Deficiency (CVID). *BMC Bioinformatics* **6,** 168
23. Villén, J., Beausoleil, S. A., Gerber, S. A., and Gygi, S. P. (2007) Large-scale phosphorylation analysis of mouse liver. *Proc. Natl. Acad. Sci. U.S.A.* **104,** 1488–1493
24. Gustafson-Wagner, E. A., Sinn, H. W., Chen, Y. L., Wang, D. Z., Reiter, R. S., Lin, J. L., Yang, B., Williamson, R. A., Chen, J., Lin, C. I., and Lin, J. J. (2007) Loss of mXinalpha, an intercalated disk protein, results in cardiac hypertrophy and cardiomyopathy with conduction defects. *Am. J. Physiol. Heart Circ. Physiol.* **293,** H2680–2692
25. Shioi, T., McMullen, J. R., Tarnavski, O., Converso, K., Sherwood, M. C., Manning, W. J., and Izumo, S. (2003) Rapamycin attenuates load-induced cardiac hypertrophy in mice. *Circulation* **107,** 1664–1670
26. Purcell, N. H., Wilkins, B. J., York, A., Saba-El-Leil, M. K., Meloche, S., Robbins, J., and Molkentin, J. D. (2007) Genetic inhibition of cardiac ERK1/2 promotes stress-induced apoptosis and heart failure but has no effect on hypertrophy in vivo. *Proc. Natl. Acad. Sci. U.S.A.* **104,** 14074–14079
27. Trinidad, J. C., Thalhammer, A., Specht, C. G., Lynn, A. J., Baker, P. R., Schoepfer, R., and Burlingame, A. L. (2008) Quantitative analysis of synaptic phosphorylation and protein expression. *Mol. Cell. Proteomics* **7,** 684–696
28. Koss, K. L., and Kranias, E. G. (1996) Phospholamban: a prominent regulator of myocardial contractility. *Circ. Res.* **79,** 1059–1063
29. Dostanic, I., Schultz Jel, J., Lorenz, J. N., and Lingrel, J. B. (2004) The alpha 1 isoform of Na,K-ATPase regulates cardiac contractility and functionally interacts and co-localizes with the Na/Ca exchanger in heart. *J. Biol. Chem.* **279,** 54053–54061
30. Morrison, L. E., Hoover, H. E., Thuerauf, D. J., and Glembotski, C. C. (2003)

ASBMB MOLECULAR & CELLULAR PROTEOMICS MCP

Mimicking phosphorylation of alphaB-crystallin on serine-59 is necessary and sufficient to provide maximal protection of cardiac myocytes from apoptosis. *Circ. Res.* **92,** 203–211
31. Charette, S. J., Lavoie, J. N., Lambert, H., and Landry, J. (2000) Inhibition of Daxx-mediated apoptosis by heat shock protein 27. *Mol. Cell. Biol.* **20,** 7602–7612
32. Huang, C. H., Wang, J. S., Chiang, S. C., Wang, Y. Y., Lai, S. T., and Weng, Z. C. (2004) Brief pressure overload of the left ventricle preconditions rabbit myocardium against infarction. *Ann. Thorac. Surg.* **78,** 628–633
33. Walker, C. A., and Spinale, F. G. (1999) The structure and function of the cardiac myocyte: a review of fundamental concepts. *J. Thorac. Cardiovasc. Surg.* **118,** 375–382
34. Kranias, E. G., and Hajjar, R. J. (2012) Modulation of cardiac contractility by the phospholamban/SERCA2a regulatome. *Circ. Res.* **110,** 1646–1660
35. Toyofuku, T., Curotto Kurzydlowski, K., Narayanan, N., and MacLennan, D. H. (1994) Identification of Ser38 as the site in cardiac sarcoplasmic reticulum Ca(2+)-ATPase that is phosphorylated by Ca2+/calmodulin-dependent protein kinase. *J. Biol. Chem.* **269,** 26492–26496
36. Hoshijima, M. (2006) Mechanical stress-strain sensors embedded in cardiac cytoskeleton: Z disk, titin, and associated structures. *Am. J. Physiol. Heart Circ. Physiol.* **290,** H1313–1325
37. Wang, Q., Lin, J. L., Wu, K. H., Wang, D. Z., Reiter, R. S., Sinn, H. W., Lin, C. I., and Lin, C. J. (2012) Xin proteins and intercalated disc maturation, signaling and diseases. *Front. Biosci.* **17,** 2566–2593
38. Kvakan, H., Kleinewietfeld, M., Qadri, F., Park, J. K., Fischer, R., Schwarz, I., Rahn, H. P., Plehm, R., Wellner, M., Elitok, S., Gratze, P., Dechend, R., Luft, F. C., and Muller, D. N. (2009) Regulatory T cells ameliorate angiotensin II-induced cardiac damage. *Circulation* **119,** 2904–2912
39. Kimura, K., Ieda, M., Kanazawa, H., Yagi, T., Tsunoda, M., Ninomiya, S., Kurosawa, H., Yoshimi, K., Mochizuki, H., Yamazaki, K., Ogawa, S., and Fukuda, K. (2007) Cardiac sympathetic rejuvenation: a link between nerve function and cardiac hypertrophy. *Circ. Res.* **100,** 1755–1764
40. Gupta, S., Purcell, N. H., Lin, A., and Sen, S. (2002) Activation of nuclear factor-kappaB is necessary for myotrophin-induced cardiac hypertrophy. *J. Cell Biol.* **159,** 1019–1028
41. Chen, L., Hahn, H., Wu, G., Chen, C. H., Liron, T., Schechtman, D., Cavallaro, G., Banci, L., Guo, Y., Bolli, R., Dorn, G. W., 2nd, and Mochly-Rosen, D. (2001) Opposing cardioprotective actions and parallel hypertrophic effects of delta PKC and epsilon PKC. *Proc. Natl. Acad. Sci. U.S.A.* **98,** 11114–11119
42. Qi, X., Disatnik, M. H., Shen, N., Sobel, R. A., and Mochly-Rosen, D. (2011) Aberrant mitochondrial fission in neurons induced by protein kinase C{delta} under oxidative stress conditions in vivo. *Mol. Biol. Cell* **22,** 256–265
43. Pitts, K. R., Yoon, Y., Krueger, E. W., and McNiven, M. A. (1999) The dynamin-like protein DLP1 is essential for normal distribution and morphology of the endoplasmic reticulum and mitochondria in mammalian cells. *Mol. Biol. Cell* **10,** 4403–4417
44. Smirnova, E., Griparic, L., Shurland, D. L., and van der Bliek, A. M. (2001) Dynamin-related protein Drp1 is required for mitochondrial division in mammalian cells. *Mol. Biol. Cell* **12,** 2245–2256
45. Liesa, M., Palacin, M., and Zorzano, A. (2009) Mitochondrial dynamics in mammalian health and disease. *Physiol. Rev.* **89,** 799–845
46. Taguchi, N., Ishihara, N., Jofuku, A., Oka, T., and Mihara, K. (2007) Mitotic phosphorylation of dynamin-related GTPase Drp1 participates in mitochondrial fission. *J. Biol. Chem.* **282,** 11521–11529
47. Cui, M., Tang, X., Christian, W. V., Yoon, Y., and Tieu, K. (2010) Perturbations in mitochondrial dynamics induced by human mutant PINK1 can be rescued by the mitochondrial division inhibitor mdivi-1. *J. Biol. Chem.* **285,** 11740–11752
48. Wang, X., Su, B., Lee, H. G., Li, X., Perry, G., Smith, M. A., and Zhu, X. (2009) Impaired balance of mitochondrial fission and fusion in Alzheimer's disease. *J. Neurosci.* **29,** 9090–9103
49. Cho, D. H., Nakamura, T., Fang, J., Cieplak, P., Godzik, A., Gu, Z., and Lipton, S. A. (2009) S-nitrosylation of Drp1 mediates beta-amyloid-related mitochondrial fission and neuronal injury. *Science* **324,** 102–105
50. Song, W., Chen, J., Petrilli, A., Liot, G., Klinglmayr, E., Zhou, Y., Poquiz, P., Tjong, J., Pouladi, M. A., Hayden, M. R., Masliah, E., Ellisman, M., Rouiller, I., Schwarzenbacher, R., Bossy, B., Perkins, G., and Bossy-Wetzel, E. (2011) Mutant huntingtin binds the mitochondrial fission GTPase dynamin-related protein-1 and increases its enzymatic activity. *Nat. Med.* **17,** 377–382
51. Ong, S. B., Subrayan, S., Lim, S. Y., Yellon, D. M., Davidson, S. M., and Hausenloy, D. J. (2010) Inhibiting mitochondrial fission protects the heart against ischemia/reperfusion injury. *Circulation* **121,** 2012–2022
52. Cassidy-Stone, A., Chipuk, J. E., Ingerman, E., Song, C., Yoo, C., Kuwana, T., Kurth, M. J., Shaw, J. T., Hinshaw, J. E., Green, D. R., and Nunnari, J. (2008) Chemical inhibition of the mitochondrial division dynamin reveals its role in Bax/Bak-dependent mitochondrial outer membrane permeabilization. *Dev. Cell* **14,** 193–204
53. Nakagawa, O., Ogawa, Y., Itoh, H., Suga, S., Komatsu, Y., Kishimoto, I., Nishino, K., Yoshimasa, T., and Nakao, K. (1995) Rapid transcriptional activation and early mRNA turnover of brain natriuretic peptide in cardiocyte hypertrophy. Evidence for brain natriuretic peptide as an "emergency" cardiac hormone against ventricular overload. *J. Clin. Invest.* **96,** 1280–1287
54. Frank, S., Gaume, B., Bergmann-Leitner, E. S., Leitner, W. W., Robert, E. G., Catez, F., Smith, C. L., and Youle, R. J. (2001) The role of dynamin-related protein 1, a mediator of mitochondrial fission, in apoptosis. *Dev. Cell* **1,** 515–525
55. Sansbury, B. E., Riggs, D. W., Brainard, R. E., Salabei, J. K., Jones, S. P., and Hill, B. G. (2011) Responses of hypertrophied myocytes to reactive species: implications for glycolysis and electrophile metabolism. *Biochem. J.* **435,** 519–528
56. Vahebi, S., Ota, A., Li, M., Warren, C. M., de Tombe, P. P., Wang, Y., and Solaro, R. J. (2007) p38-MAPK induced dephosphorylation of alpha-tropomyosin is associated with depression of myocardial sarcomeric tension and ATPase activity. *Circ. Res.* **100,** 408–415
57. Kumarapeli, A. R., Su, H., Huang, W., Tang, M., Zheng, H., Horak, K. M., Li, M., and Wang, X. (2008) Alpha B-crystallin suppresses pressure overload cardiac hypertrophy. *Circ. Res.* **103,** 1473–1482
58. Clerk, A., Bogoyevitch, M. A., Anderson, M. B., and Sugden, P. H. (1994) Differential activation of protein kinase C isoforms by endothelin-1 and phenylephrine and subsequent stimulation of p42 and p44 mitogen-activated protein kinases in ventricular myocytes cultured from neonatal rat hearts. *J. Biol. Chem.* **269,** 32848–32857
59. Li, J. M., and Brooks, G. (1999) Cell cycle regulatory molecules (cyclins, cyclin-dependent kinases and cyclin-dependent kinase inhibitors) and the cardiovascular system; potential targets for therapy? *Eur. Heart J.* **20,** 406–420
60. Han, X. J., Lu, Y. F., Li, S. A., Kaitsuka, T., Sato, Y., Tomizawa, K., Nairn, A. C., Takei, K., Matsui, H., and Matsushita, M. (2008) CaM kinase I alpha-induced phosphorylation of Drp1 regulates mitochondrial morphology. *J. Cell Biol.* **182,** 573–585
61. Wang, W., Wang, Y., Long, J., Wang, J., Haudek, S. B., Overbeek, P., Chang, B. H., Schumacker, P. T., and Danesh, F. R. (2012) Mitochondrial fission triggered by hyperglycemia is mediated by ROCK1 activation in podocytes and endothelial cells. *Cell Metab.* **15,** 186–200
62. Cribbs, J. T., and Strack, S. (2007) Reversible phosphorylation of Drp1 by cyclic AMP-dependent protein kinase and calcineurin regulates mitochondrial fission and cell death. *EMBO Rep.* **8,** 939–944
63. Passier, R., Zeng, H., Frey, N., Naya, F. J., Nicol, R. L., McKinsey, T. A., Overbeek, P., Richardson, J. A., Grant, S. R., and Olson, E. N. (2000) CaM kinase signaling induces cardiac hypertrophy and activates the MEF2 transcription factor in vivo. *J. Clin. Invest.* **105,** 1395–1406
64. Higashi, M., Shimokawa, H., Hattori, T., Hiroki, J., Mukai, Y., Morikawa, K., Ichiki, T., Takahashi, S., and Takeshita, A. (2003) Long-term inhibition of Rho-kinase suppresses angiotensin II-induced cardiovascular hypertrophy in rats in vivo: effect on endothelial NAD(P)H oxidase system. *Circ. Res.* **93,** 767–775
65. Molkentin, J. D., Lu, J. R., Antos, C. L., Markham, B., Richardson, J., Robbins, J., Grant, S. R., and Olson, E. N. (1998) A calcineurin-dependent transcriptional pathway for cardiac hypertrophy. *Cell* **93,** 215–228
66. Hong, Z., Kutty, S., Toth, P. T., Marsboom, G., Hammel, J. M., Chamberlain, C., Ryan, J. J., Zhang, H. J., Sharp, W. W., Morrow, E., Trivedi, K., Weir, E. K., and Archer, S. L. (2013) Role of dynamin-related protein 1 (drp1)-mediated mitochondrial fission in oxygen sensing and constriction of the ductus arteriosus. *Circ. Res.* **112,** 802–815
67. Tsujimoto, I., Hikoso, S., Yamaguchi, O., Kashiwase, K., Nakai, A., Takeda, T., Watanabe, T., Taniike, M., Matsumura, Y., Nishida, K., Hori, M., Kogo, M., and Otsu, K. (2005) The antioxidant edaravone attenuates pressure overload-induced left ventricular hypertrophy. *Hypertension* **45,** 921–926

ASBMB MOLECULAR & CELLULAR PROTEOMICS MCP

68. Tanaka, K., Honda, M., and Takabatake, T. (2001) Redox regulation of MAPK pathways and cardiac hypertrophy in adult rat cardiac myocyte. *J. Am. Coll. Cardiol.* **37,** 676–685
69. Berridge, M. J. (2006) Remodelling Ca2+ signalling systems and cardiac hypertrophy. *Biochem. Soc. Trans.* **34,** 228–231
70. Piquereau, J., Caffin, F., Novotova, M., Prola, A., Garnier, A., Mateo, P., Fortin, D., Huynh le, H., Nicolas, V., Alavi, M. V., Brenner, C., Ventura-Clapier, R., Veksler, V., and Joubert, F. (2012) Down-regulation of OPA1 alters mouse mitochondrial morphology, PTP function, and cardiac adaptation to pressure overload. *Cardiovasc. Res.* **94,** 408–417
71. Ashrafian, H., Docherty, L., Leo, V., Towlson, C., Neilan, M., Steeples, V., Lygate, C. A., Hough, T., Townsend, S., Williams, D., Wells, S., Norris, D., Glyn-Jones, S., Land, J., Barbaric, I., Lalanne, Z., Denny, P., Szumska, D., Bhattacharya, S., Griffin, J. L., Hargreaves, I., Fernandez-Fuentes, N., Cheeseman, M., Watkins, H., and Dear, T. N. (2010) A mutation in the mitochondrial fission gene Dnm1l leads to cardiomyopathy. *PLoS Genet.* **6,** e1001000
72. McKinsey, T. A., and Kass, D. A. (2007) Small-molecule therapies for cardiac hypertrophy: moving beneath the cell surface. *Nat. Rev. Drug Discov.* **6,** 617–635

ASBMB MOLECULAR & CELLULAR PROTEOMICS MCP